Thermometry in aqueous solutions and sprays using two-color LIF and structured illumination

Mishra, Yogeshwar; Abou Nada, Fahd Jouda; Polster, Stephanie; Kristensson, Elias; Berrocal, Edouard

Published in:
Optics Express

DOI:
10.1364/OE.24.004949

2016

Thermometry in aqueous solutions and sprays using two-color LIF and structured illumination

Yogeshwar Nath Mishra,[1]* Fahed Abou Nada,[1] Stephanie Polster,[2] Elias Kristensson[1] and Edouard Berrocal[1, 2]

[1]*Division of Combustion Physics, Physics Department, Lund University, Box 118, Lund 22100, Sweden*
[2]*SAOT, Institute of Engineering Thermodynamics, Friedrich-Alexander-University Erlangen-Nuremberg, Germany*
[*]*yogeshwar.mishra@forbrf.lth.se*

Abstract: In imaging, the detection of light originating from multiple scattering, indirect reflections and surrounding backgrounds are known to produce errors especially in intensity-ratio based measurements. SLIPI (Structured Laser Illumination Planar Imaging) is an imaging technique that significantly reduces the impact of such issues. In this study, SLIPI is combined with the two-color LIF (Laser Induced Fluorescence) ratio thermometry approach for measuring water temperature in both a cuvette and a hollow-cone spray. By removing the unwanted background interferences using SLIPI, we observe both significant improvements in terms of temperature sensitivity as well as more pronounced temperature gradients within the spray.

OCIS codes: (120.4820) Optical systems; (110.0110) Imaging systems; (120.6780) Temperature; (300.2530) Fluorescence, laser-induced; (290.4210) Multiple scattering.

References and links

1. C. Gosse, C. Bergaud, and P. Löw, "Molecular Probes for Thermometry in Microfluidic Devices," in *Thermal Nanosystems and Nanomaterials, Topics in Advanced Physics*, S. Volz ed., Sprin.-Verl., **118**, 301–341 (2009).
2. P. R. N. Childs, J. R. Greenwood, and C. A. Long, "Review of temperature measurement," Rev. Sci. Instrum. **71**(8), 2959–2978 (2000).
3. F. Lemoine and G. Castanet, "Temperature and chemical composition of droplets by optical measurement techniques: a state-of-the-art review," Exp. Fluids **54**(7), 1572 (2013).
4. X. Wu, H. Jiang, Y. Wu, J. Song, G. Gréhan, S. Saengkaew, L. Chen, X. Gao, and K. Cen, "One-dimensional rainbow thermometry system by using slit apertures," Opt. Lett. **39**(3), 638–641 (2014).
5. R. F. Hankel, A. Günther, K. E. Wirth, A. Leipertz, and A. Braeuer, "Liquid phase temperature determination in dense water sprays using linear Raman scattering," Opt. Express **22**(7), 7962–7971 (2014).
6. J. Coppeta and C. Rogers, "Dual emission laser induced fluorescence for direct planar scalar behavior measurements," Exp. Fluids **25**(1), 1–15 (1998).
7. M. Coolen, R. Kieft, C. Rindt, and A. Van Steenhoven, "Applications of 2D LIF temperature measurements in water using a Nd:YAG laser," Exp. Fluids **27**(5), 420–426 (1999).
8. J. Sakakibara and R. Adrian, "Whole field measurements of temperature in water using two-color laser-induced fluorescence," Exp. Fluids **26**(1-2), 7–15 (1999).
9. V. K. Natrajan and K. T. Christensen, "Two-color laser-induced fluorescent thermometry for microfluidic systems," Meas. Sci. Technol. **20**(1), 015401 (2009).
10. P. Lavieille, F. Lemoine, G. Lavergne, and M. Lebouché, "Evaporating and combusting droplet temperature measurements using two-color laser-induced fluorescence," Exp. Fluids **31**(1), 45–55 (2001).
11. G. Castanet, P. Lavieille, F. Lemoine, and M. Lebouché, "Measurement of the temperature distribution within monodisperse combusting droplets in linear streams using two-color laser-induced fluorescence," Exp. Fluids **35**, 563–571 (2003).
12. M. Bruchhausen, F. Guillard, and F. Lemoine, "Instantaneous measurement of two-dimensional temperature distributions by means of two-color planar laser induced fluorescence (PLIF)," Exp. Fluids **38**(1), 123–131 (2005).
13. M. Wolff, A. Delconte, F. Schmidt, P. Gucher, and F. Lemoine, "High-pressure diesel spray temperature measurements using two-colour laser induced fluorescence," Meas. Sci. Technol. **18**(3), 697–706 (2007).
14. I. Düwel, H. W. Ge, H. Kronemayer, R. Dibble, E. Gutheil, C. Schulz, and J. Wolfrum, "Experimental and numerical characterization of a turbulent spray flame," Proc. Combust. Inst. **31**(2), 2247–2255 (2007).
15. M. R. Vetrano, A. Simonini, J. Steelant, and R. Rambaud, "Thermal characterization of a flashing jet by planar laser-induced fluorescence," Exp. Fluids **54**(7), 1573–1583 (2013).

#253552 Received 9 Nov 2015; revised 10 Feb 2016; accepted 14 Feb 2016; published 26 Feb 2016

16. R. P. C. Zegers, M. Yu, C. Bekdemir, N. J. Dam, C. C. M. Luijten, and L. P. H. de Goey, "Temperature measurements of the gas-phase during surrogate diesel injection using two-color toluene LIF," Appl. Phys. B **112**(1), 7–23 (2013).
17. A. Labergue, A. Delconte, G. Castanet, and F. Lemoine, "Study of the droplet size effect coupled with the laser light scattering in sprays for two-color LIF thermometry measurements," Exp. Fluids **52**(5), 1121–1132 (2012).
18. L. Perrin, G. Castanet, and F. Lemoine, "Characterization of the evaporation of interacting droplets using combined optical techniques," Exp. Fluids **56**(29), 1–16 (2015).
19. A. Omrane, G. Särner, and M. Aldén, "2D-temperature imaging of single droplets and sprays using thermographic phosphors," Appl. Phys. B **79**(4), 431–434 (2004).
20. J. Brübach, A. Patt, and A. Dreizler, "Spray thermometry using thermographic phosphors," Appl. Phys. B **83**(4), 499–502 (2006).
21. G. Lamanna, H. Kamoun, B. Arnold, K. Schlottke, B. Weigand, and J. Steelant, "Differential infrared thermography (DIT) in a flashing jet: a feasibility study," Quantum Infrared Therm. J. **10**(1), 112–131 (2013).
22. H. Golzke, P. Leick, and A. Dreizler, "Differential infrared thermography of gasoline direct injection sprays," Quantum Infrared Therm. J. **12**, 1–20 (2015).
23. Y. N. Mishra, E. Kristensson, and E. Berrocal, "Reliable LIF/Mie droplet sizing in sprays using structured laser illumination planar imaging," Opt. Express **22**(4), 4480–4492 (2014).
24. M. A. A. Neil, R. Juskaitis, and T. Wilson, "Method of obtaining optical sectioning by using structured light in a conventional microscope," Opt. Lett. **22**(24), 1905–1907 (1997).
25. E. Berrocal, E. Kristensson, M. Richter, M. Linne, and M. Aldén, "Application of structured illumination for multiple scattering suppression in planar laser imaging of dense sprays," Opt. Express **16**(22), 17870–17881 (2008).
26. E. Kristensson, E. Berrocal, M. Richter, S. G. Pettersson, and M. Aldén, "High-speed structured planar laser illumination for contrast improvement of two-phase flow images," Opt. Lett. **33**(23), 2752–2754 (2008).
27. E. Berrocal, J. Johnsson, E. Kristensson, and M. Aldén, "Single scattering detection in turbid media using single-phase structured illumination filtering," J. Euro. Opt. Soc. Rap. Pub. **7**, 12015 (2012).
28. E. Kristensson, E. Berrocal, and M. Aldén, "Two-pulse structured illumination imaging," Opt. Lett. **39**(9), 2584–2587 (2014).
29. J. Sutton, B. Fisher, and J. Fleming, "A laser-induced fluorescence measurement for aqueous fluid flows with improved temperature sensitivity," Exp. Fluids **45**(5), 869–881 (2008).
30. S. Polster, Temperature mapping of liquids using two-colour LIF ratio and SLIPI: Application for spray thermometry (Master Thesis, University of Erlangen-Nuremberg, 2014).
31. E. Kristensson, A. Ehn, J. Bood, and M. Aldén, "Advancements in Rayleigh scattering thermometry by means of structured illumination," Proc. Combust. Inst. **35**(3), 3689–3696 (2015).
32. P. Lavieille, A. Delconte, D. Blondel, M. Lebouché, and F. Lemoine, "Non-intrusive temperature measurements using three-color laser-induced fluorescence," Exp. Fluids **36**, 706–716 (2004).

1. Introduction

Temperature measurement of fluids is of great importance for various industrial applications. Assessing temperature fields not only help to optimize the system design, but also to maximize efficiency. For example, in microfluidics systems, chemical reactivity can be optimized if the local temperature of the fluid is known [1]. Also, by measuring the temperature in microfluidics-based microelectromechanical system (MEMS) thermal transport management can be greatly improved. In spray systems, the ability to control droplet evaporation is highly desired, especially in liquid fuel combustion devices as well as for spray cooling/drying applications. In internal combustion engines, droplets are required to evaporate on the order of milliseconds in order to form the adequate fuel/air mixture proportion prior to ignition. In spray cooling, a spatially uniform cooling is usually desired. However, the heat transport phenomenon in sprays is quite complex and one would need to determine droplets temperature with great accuracy for the detail study of spray evaporation. Several non-contact (e.g. optical) and contact (e.g. thermocouples) methods have been reported to measure temperature of liquids and sprays [2,3]. Optical techniques are often preferred because of their non-intrusive nature and various methods, such as Rainbow Refractometry, Raman scattering, Laser-Induced Exciplex Fluorescence (LIEF), Laser-Induced Fluorescence (LIF) and Laser-Induced Phosphorescence (LIP) have been applied for thermometry in liquids, droplets and spray systems [3].

The Global Rainbow Refractrometry (GRR) deduces temperature by correlating it with droplets refractive index. However, the technique relies on point-scanning and, hence, assessing the temperature field in 2D becomes a time-consuming process. In addition, the

#253552 Received 9 Nov 2015; revised 10 Feb 2016; accepted 14 Feb 2016; published 26 Feb 2016

presence of non-spherical droplets can give large measurement uncertainties. As an extension of GRR, a rainbow thermometry arrangement capable of acquiring data along a line has recently been developed and demonstrated [4]. Another point-measurement scheme is the linear Raman scattering, which can provide the liquid phase temperature of a spray from the OH-stretching vibration band of water. This approach has been recently used for extracting the droplet temperature in superheated and cold water sprays [5].

In opposition to point-wise measurements, temperature measurement techniques based laser sheet illumination are very attractive as they may provide spatially resolved temperature maps. The two-color LIF ratio method has been extensively used over the past years for liquid- and gas thermometry [6–18]. In order to apply it, one or more dyes are judiciously selected, each producing a temperature sensitive spectral shift in their emitted LIF signals when excited at an appropriate wavelength. The two-color ratio approach with a single dye is usually preferred as it eliminates issues related to changes in dye concentration, laser intensity fluctuations, light extinction *etc* [10–18]. Lemoine and associates pioneered this method for thermometry in droplet streams and sprays [10–13,17,18].

Planar LIEF assess liquid temperature by taking the intensity ratio of exciplex and monomer signals. Despite its ability of distinguishing between the liquid/vapor phases it is limited to applications in oxygen-free environments in order to avoid exciplex quenching, thus making it challenging to implement in practical combustion devices.

LIP thermometry can be performed by exploiting the temperature dependence in either the lifetime- or the spectral characteristics of the phosphorescence signal. The main advantages of using LIP thermometry are that thermographic phosphors are tolerant to harsh combustion situations (such as in combustion engines) as well as being capable of measuring temperatures up to 2000 K. Unlike many dye tracers used for LIF thermometry, thermographic phosphors usually display a luminescence that is independent of pressure- and oxygen quenching. However, even though the technique has been demonstrated for thermometry in single droplets and sprays [19,20], the use of phosphor powders (solid particles in the range of a few microns in size) are undesired as they do affect the atomization process especially if the particles aggregate.

Finally, the Differential Infrared Thermometry (DIT) technique [21,22] enables the 2D measurement of the spray infrared emissivity. The temperatures across the spray are then determined using the Planck's radiation law.

A common measurement obstacle for all techniques described above when applied for spray diagnostics concerns effects introduced by multiple light scattering. In a recent article [23], Mishra *et al.* have demonstrated that removing the contribution of multiply scattered light using SLIPI significantly improve the measurement accuracy when assessing the droplet Sauter Mean Diameter (SMD) through the ratio of LIF/Mie-scattering. In this report, we address the issues associated with multiple light scattering in temperature measurements, for the first time, by combining SLIPI with two-color LIF ratio thermometry. The approach is first demonstrated in a transparent cuvette for water temperatures ranging from 25°C to 85°C and then applied to a pressure swirl atomizing spray set at 20 bar liquid injection pressure and at temperatures from 25°C to 55°C. At such operating conditions the spray remains fairly dilute with an optical depth of OD ≈1 (as shown in [23]). The effects of dye concentration and laser power on the SLIPI-LIF ratio are also investigated. Finally, for both cases of study, the LIF ratio is calibrated using thermocouple measurements.

2. Description of the imaging techniques

2.1 Two-color LIF ratio thermometry

Certain fluorescing dyes are known to display spectral variations in their LIF emission depending on their temperature – a phenomenon the two-color LIF ratio technique exploits for thermometry. The technique is based on recording the LIF emission within two suitable

#253552 Received 9 Nov 2015; revised 10 Feb 2016; accepted 14 Feb 2016; published 26 Feb 2016

spectral bands, I_{LIF1} and I_{LIF1}, using bandpass filters and to calculate the temperature-sensitive intensity ratio between these signal components. One experimental challenge associated with the technique concerns background contributions, which may stem from multiply scattered light, indirect reflections or other undesired out-of-focus light. Therefore, since two different spectral bands are studied, the background contribution (*BG*) in each signal (S_{LIF}) will, unavoidably, be different. This difference will consequently influence value of the intensity ratio R which is extracted in order to evaluate the temperature, according to:

$$R(T) = \frac{I_{LIF2}}{I_{LIF1}} = \frac{S_{LIF2} - BG_2}{S_{LIF1} - BG_1} \tag{1}$$

The background light is commonly approximated by recording an image while having no laser excitation, yet such a procedure does not take all sources of noises into consideration. By not correcting for the effects introduced by multiple light scattering the resulting ratio can be strongly influenced (as demonstrated in [23]). Applying SLIPI provides means to distinguish between signal components and background interferences and to suppress the later, as illustrated in Fig. 1.

2.2 Structured Laser Illumination Planar Imaging

SLIPI is a technique inspired from structured illumination microscopy [24] and was developed in order to imaging optically dense spray where the majority of photons leaving the medium have undergone multiple scattering events [25,26]. It is based on using a laser sheet where the light intensity profile is following a sinusoidal pattern. The resulting "lines pattern" is vertically shifted by a spatial phase difference of 120° in between the recordings of two successive sub-images as shown in Fig. 1(a). The spatial modulation serves the purpose of "tagging" the singly scattered photons, as photons which scatter multiple times forget this signature before reaching the detector. Using a sinusoidal line structure, the resultant intensity of the image $I(x, y)$ is described as:

$$I(x, y) = I_C(x, y) + I_S(x, y) \cdot \sin(2\pi x\nu + \phi) \tag{2}$$

Where ν represents the modulation frequency and ϕ the spatial phase. Here, $I_C(x, y)$ is the intensity corresponding to singly and multiply scattered photons while, $I_S(x, y)$ represent the amplitude of the modulation which is the signature of the singly scattered photons. In order to deduce $I_S(x, y)$ over the full image the root-mean square of three sub-images I_0, I_{120}, and I_{240} is calculated:

$$I_S = \frac{\sqrt{2}}{3} \cdot \left[(I_0 - I_{120})^2 + (I_0 - I_{240})^2 + (I_{120} - I_{240})^2 \right]^{1/2} \tag{3}$$

By instead averaging those three sub-images a conventional light sheet image corresponding to $I_C(x, y)$ can be deduced:

$$I_C = \left[I_0 + I_{120} + I_{240} \right] / 3 \tag{4}$$

In this article, images corresponding to $I_C(x, y)$ and to $I_S(x, y)$ will be denoted CONV and SLIPI, respectively.

#253552 Received 9 Nov 2015; revised 10 Feb 2016; accepted 14 Feb 2016; published 26 Feb 2016

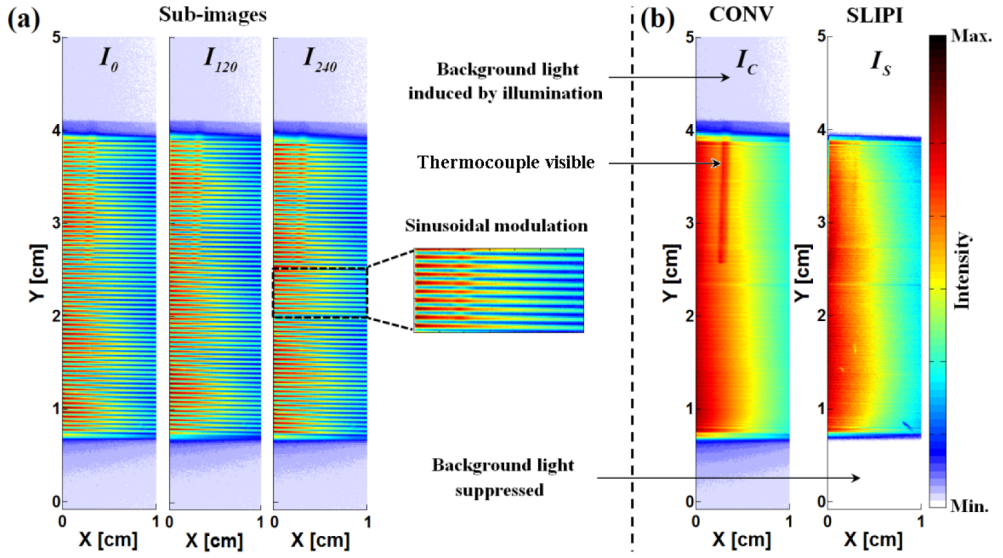

Fig. 1. Illustration of the SLIPI approach: A light sheet having an intensity-modulated pattern along the vertical direction is crossing a cuvette with fluorescing liquid. (a) shows the three sub-images where the "lines pattern" is vertically shifted one third of the spatial period. (b) shows the conventional laser sheet and the SLIPI images which have been constructed using the three sub-images. It is seen here that background interferences induced by the incident illumination is efficiently suppressed by means of SLIPI (see also the suppression of the thermocouple visibility which is located just behind the light sheet).

To obtain single-shot data, it is possible to estimate $I_S(x,y)$ from a single sub-image, albeit at the cost of image resolution [27]. A second option, that has recently been experimentally verified, is to use two phase-mismatched sub-images of high frequency and to extract the absolute value of their intensity difference which also provides an estimate of $I_S(x,y)$ at nearly full image resolution [28].

3. Description of the experiments

3.1 Optical characteristics of Fluorescein

A concentrated solution of Fluorescein dye (7% by weight) served as a temperature sensitive tracer and was mixed with water (pH~7). Fluorescein is a biodegradable dye, characterized by a high quantum yield. Sutton *et al.* have demonstrated that fluorescein 27 has a positive temperature sensitivity (3.5%/°C), significantly higher than Rhodamine B and Kiton Red (–1.59%/°C) for an excitation wavelength of 532 nm [29]. The absorption spectrum of the Fluorescein dye solution used here is given in Fig. 2(a) (recorded using a photo-spectrometer T60U, PG Instruments) showing a maximum absorption at 485 nm, as well as some additional absorption peaks at 236 nm and 200 nm. The molecular structure of the dye is depicted in Fig. 2(b).

The temperature-dependent LIF spectrum of the solution (dye/water) is investigated at an excitation wavelength of λ = 447 nm and at temperatures ranging from 21°C to 90°C. The spectra are recorded using a spectrometer AvaSpec-USB2 while the temperature is monitored using a K-type thermocouple (see [30] for details). The non-normalized spectra, shown in Fig. 3(a), indicate that the maximum fluorescence intensity reached at 21°C decreases by 27.3% at 90°C. When normalizing the spectra, Fig. 3(b), a red-shift of the intensity maximum from 523 nm to 530 nm is clearly observed.

#253552 Received 9 Nov 2015; revised 10 Feb 2016; accepted 14 Feb 2016; published 26 Feb 2016

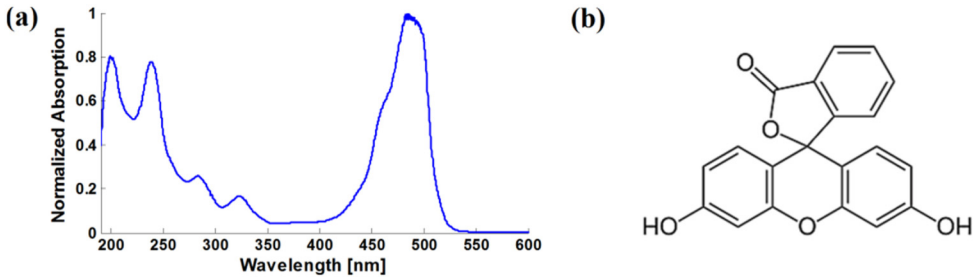

Fig. 2. (a) Absorption spectrum of Fluorescein dye dissolved in water. (b) Molecular structure of Fluorescein (from Ref. [30].

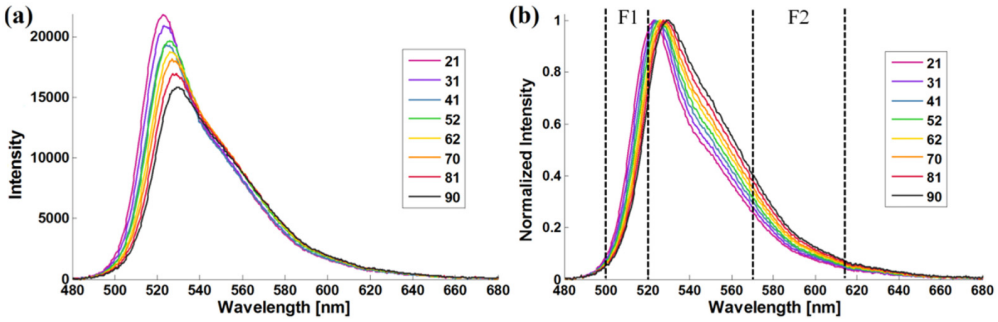

Fig. 3. Non-normalized in (a) and normalized in (b) LIF emission spectra of the Fluorescein dye at 447 nm excitation and for a temperature ranging between 21°C and 90°C: A change in LIF emission intensity and spectral shift are apparent. The spectral range of two selected optical filters (F1, F2), used for the LIF ratio (see section 3.2) is also indicated in (b).

3.2 Temperature sensitivity for different spectral band ratios

Using the spectra presented in Fig. 3, two spectral bands need to be selected to achieve optimum measurement sensitivity without compromising too much on the signal level. Three cases have been identified and evaluated:

- Case A represents the spectral band ratio against temperature for two bands selected for maximum intensity.
- Case B represents the spectral band ratio against temperature for maximum temperature sensitivity.
- Case C represents the optimized bands which have been selected in the experiment, being a trade-off between good intensity signal and temperature sensitivity.

A plot of the normalized ratio against the temperature is shown in Fig. 4 for the three different cases. Here, the exact central wavelengths are expressed as λ_{LIF1}, λ_{LIF2} and full-width at half maxima (FWHM) as Δ_{LIF1}, Δ_{LIF2} for first bands and second bands, respectively. The maximum signal intensity can be achieved in case A if the spectral band ratio is extracted using a first band λ_{LIF1} = 515 nm; Δ_{LIF1} = 20 nm and a second band λ_{LIF2} = 575 nm; Δ_{LIF2} = 80 nm. For maximum sensitivity, in case B, the first band should correspond to λ_{LIF1} = 507.5 nm; Δ_{LIF1} = 5 nm and second band to λ_{LIF2} = 612.5 nm; Δ_{LIF2} = 5 nm. However, the FWHM bands cover, for case B, only 5 nm which would significantly reduce the amount of signal that would be detected experimentally. Hence, reasonably large bands have to be selected. The ratio C extracted from a first band λ_{LIF1} = 510 nm, Δ_{LIF1} = 20 nm and a second band λ_{LIF2} = 592 nm, Δ_{LIF2} = 43 nm has been found to be a suitable compromise. The spectral width of these bands is denoted F1 and F2 respectively, and can be seen in the Fig. 3(b). The

#253552 Received 9 Nov 2015; revised 10 Feb 2016; accepted 14 Feb 2016; published 26 Feb 2016

corresponding filters are high performance optical bandpass filters from Edmund Optics, with a transmission superior to 93% and a blocking at optical density of above 6.

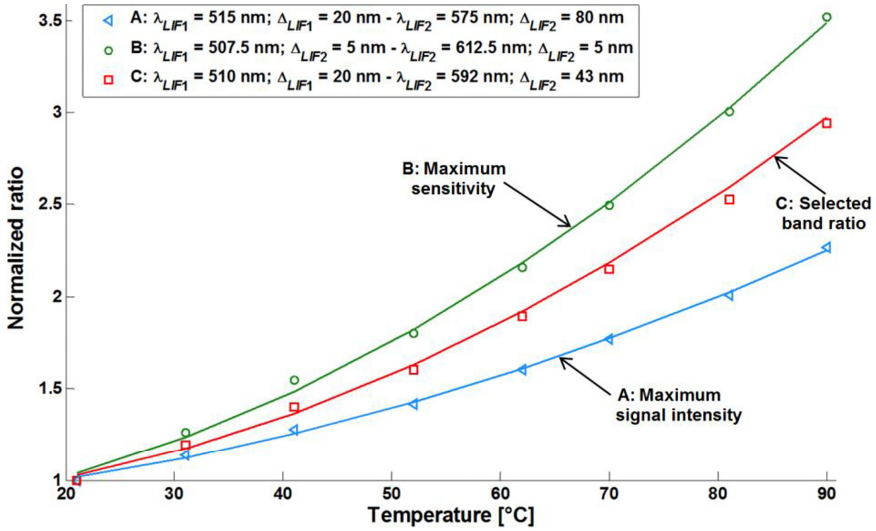

Fig. 4. Normalized ratio of signal intensity against temperature for different band ratios, evaluated through computational calculations. The solid lines are second-order polynomial fittings of the respective markers.

3.3 SLIPI two-color LIF ratio: experimental setup

A schematic setup of the combined SLIPI two-color LIF ratio technique is shown in Fig. 5. A spatially modulated laser light sheet (52 mm height,~0.5 mm thickness) is created from the SLIPI setup using a 447 nm continuous wave diode laser. This illumination scheme excites the dyed solution through either a cuvette or a hollow-cone water spray. The emitted fluorescing signal is detected by two electron multiplying CCD cameras of the same characteristics. Each of these 14-bit cameras (Andor, Luca R) records an image of 1004 × 1002 pixels. To record the two LIF signals simultaneously, a beam splitter (40/60%: transmission/reflection) is used in-between the cameras together with two high performance bandpass filters, F1 and F2 (see characteristics in the section 3.2) fixed in front of each objective. The overlap of the cameras field-of-view is accurately adjusted by imaging a test target and by using a warping scheme to ensure a perfect pixel to pixel overlapping. For correlating the two-color LIF ratio with liquid temperature, a calibration work is performed by measuring temperature within a define region on the recorded image. The reference temperature is measured using a thermocouple of 1 mm tip diameter (K type, Pentronic AB). In cuvette measurements, the thermocouple is kept static and inserted within ~2 mm behind the laser sheet. In the spray case, the thermocouple is inserted into the light sheet directly and for each measured temperature (droplet temperature in this case) the LIF images are recorded after rapid removal of the thermocouple. As the studied spray is steady (continuously running for a given temperature of the injected water), the assumption that the temperature remains constant between the thermocouple measurements and the images recordings is considered as valid.

For the cuvette measurements, the Fluorescein dye solution is mixed with water and heated up to 90°C. The two-color LIF images are then recorded from 85°C down to 25°C at every five degrees temperature change. The exposure time of the cameras is set to 12 milliseconds for each sub-image, so that the final SLIPI image is recorded in a sufficient short time where the temperature decreases less than 0.1°C for each measurement point. This is required at higher temperature conditions where the water is rapidly cooled. Moreover, in

#253552 Received 9 Nov 2015; revised 10 Feb 2016; accepted 14 Feb 2016; published 26 Feb 2016

order to have an optimized signal-to-noise ratio (SNR), the smallest f-number of the objectives is chosen, corresponding here to $f_{\#} = 2.8$.

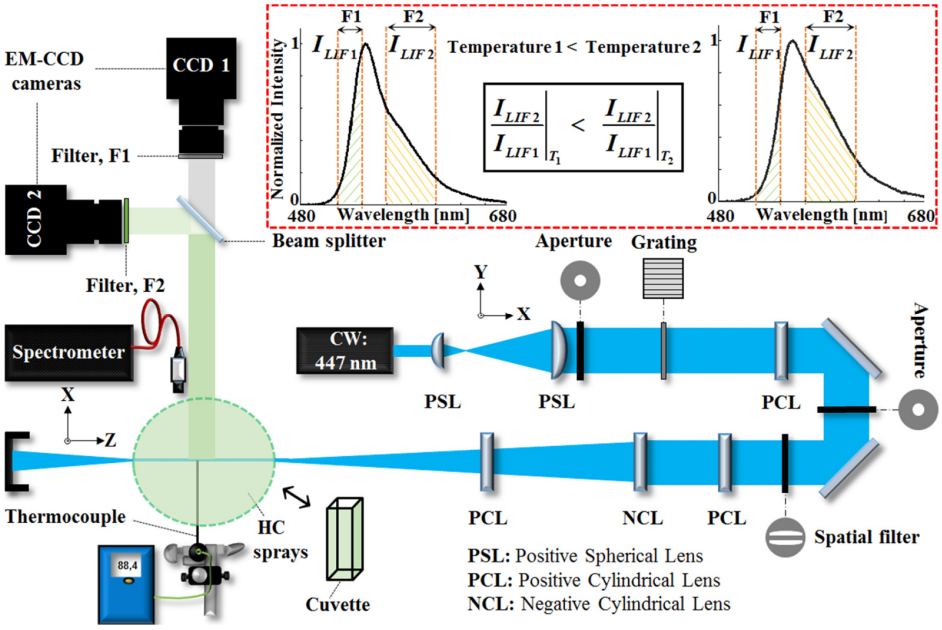

Fig. 5. Experimental setup of SLIPI two-color LIF ratio thermometry including all optical components. The dashed box (red) on the top right is an illustration of two-color LIF ratio thermometry principle.

For the spray measurements, the laser sheet is located at 1.5 cm below the nozzle tip. The dyed water is heated in a 50 liters tank before being sprayed by a pressure swirl nozzle (Lechler, no. 216.324) of 1 mm orifice diameter. A steady condition is set at 20 bars injection pressure corresponding to a liquid flow rate of 1.26 liters/min. The liquid is discharged at room temperature and atmospheric pressure conditions. The two-color LIF images are recorded for droplet temperatures ranging between 25 to 55°C with a step difference of 5°C.

4. Cuvette measurement results

4.1 Non-calibrated results

The conventional and SLIPI images of two-color LIF ratio of the cuvette measurements are given in Figs. 6(a) and 6(b), respectively. The fixed dye concentration and incident laser power of extinction coefficient (μ_e) of 1.5 cm^{-1} and 18 mW, respectively are used during the measurements. The extinction coefficient is calculated according to the transmission measurements procedure described in reference [23]. It is seen that the LIF ratio increases as liquid temperature increases from 25°C to 85°C both for the CONV and SLIPI cases. However, in Fig. 6(a), a signal is generated on the CONV images in the portions which are not excited by the laser sheet. This can be seen both on the top and bottom of the illuminated plane and is due to the contribution of the unwanted off-axis (background) fluorescence and/or reflections from the cuvette edges. This undesired signal originates from out-of-focus regions produce blurring effects in ratio images. On the other hand, SLIPI (see in Fig. 6(b) corrects for such effects, enabling collection of only the desired LIF signal. Thus, the extracted SLIPI-LIF ratio enhances the visualization of temperature gradients significantly. Moreover, in CONV, the inserted thermocouple (behind the laser sheet) is also observed, while it is significantly less apparent in SLIPI. Therefore, SLIPI can be used in situations where unwanted reflections are unavoidable [31].

#253552 Received 9 Nov 2015; revised 10 Feb 2016; accepted 14 Feb 2016; published 26 Feb 2016

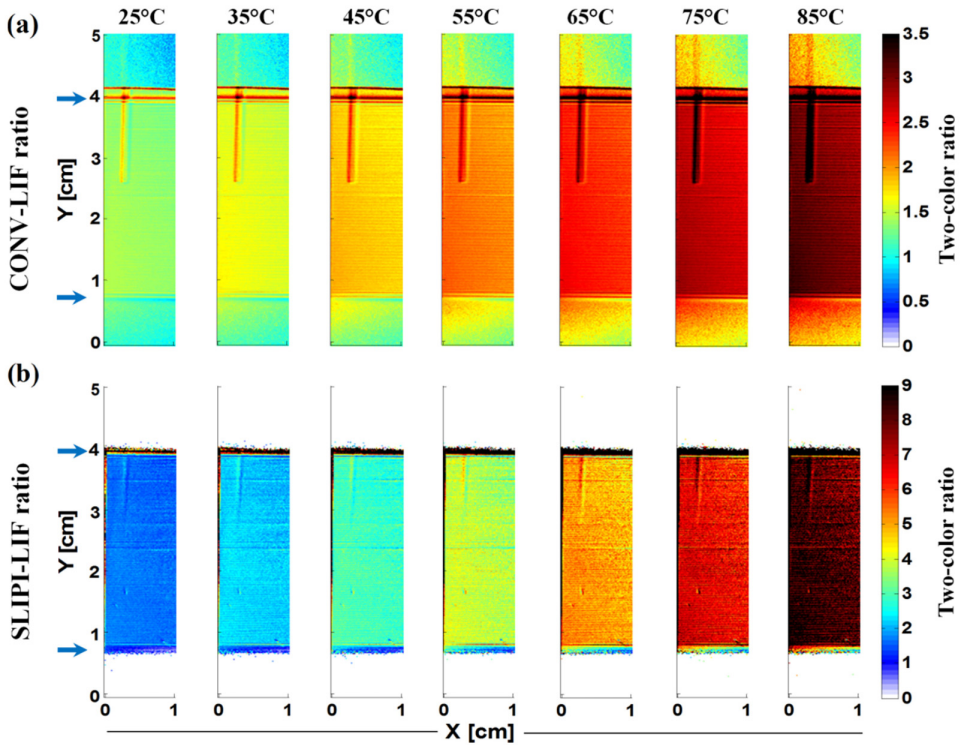

Fig. 6. Two-color LIF ratio images as a function of liquid temperature for the CONV in (a) and SLIPI in (b). The LIF ratio shows, in both cases, an increase with temperature. However, CONV, produces erroneous signals from non-illuminated portions, an artifact that is corrected in the case of SLIPI.

4.2 Calibrated results

To further compare the temperature sensitivity between CONV and SLIPI, the two-color LIF ratio and its sensitivity are plotted as a function of temperature in Figs. 7(a) and 7(b), respectively. In Fig. 7(a), the plotted curves are obtained by correlating the reference temperature with the averaged two-color LIF ratio over the thermocouple measurement region corresponding to a 100 × 100 pixels area. It is seen that the LIF ratio increases from 1.8 to 8.9 with SLIPI while it only increases from 1.4 to 3 with CONV when the temperature rises from 25°C to 85°C. Therefore, the LIF ratio dynamic range improves by a factor of three with the SLIPI technique in comparison with the conventional planar imaging approach. Note that the solid lines are third-order polynomial fittings of the respective markers.

In Fig. 7(b), the sensitivity per degree is deduced by taking the derivative of the two-color LIF ratio R with respect to the temperature T. It is seen that SLIPI offers a much higher sensitivity than CONV. From, the relative sensitivity curve, represented by the green dashed line, it is apparent that at 25°C the measurement sensitivity is more than twice as high with SLIPI than with CONV and it increases up to 4 and 6 times higher at 55°C and 85°C, respectively. Those improvements in sensitivity are mostly due to the increase of signal-to-noise ratio obtained with SLIPI.

The calibrated SLIPI-LIF ratio is shown in Fig. 8. Those images are obtained by using the SLIPI curve from Fig. 7(a) as a calibration curve and generating an image of the absolute temperature of the water in the cuvette. It is apparent from those images that the water temperature is homogeneous throughout the light sheet, for each reference temperature.

#253552 Received 9 Nov 2015; revised 10 Feb 2016; accepted 14 Feb 2016; published 26 Feb 2016

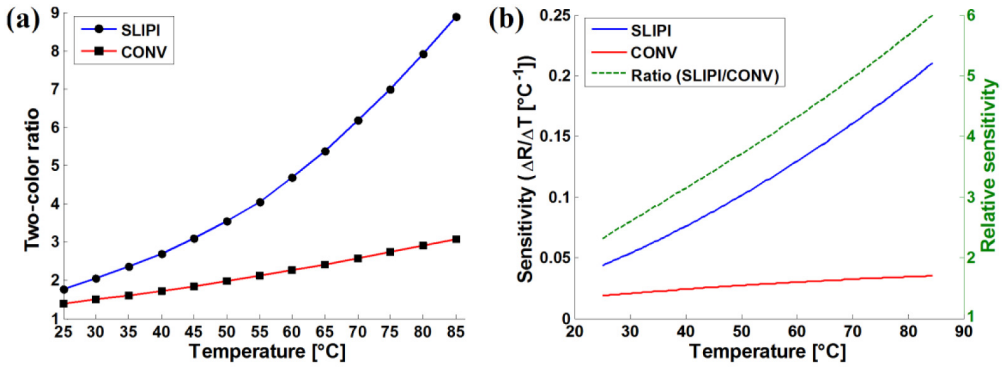

Fig. 7. (a) The two-color LIF ratio (both from CONV and SLIPI) are plotted as a function of liquid temperature. It is found that the SLIPI-LIF ratio improves the dynamics by a factor of three compared to that of CONV-LIF ratio. (b) The sensitivity per degrees (left Y-axis) both for the SLIPI and CONV is shown together with the sensitivity ratio SLIPI/CONV (right Y-axis, in green).

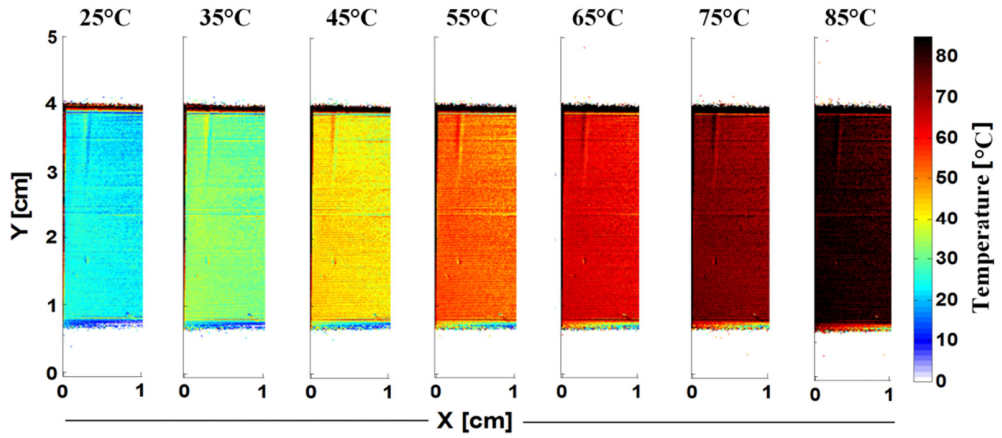

Fig. 8. Calibrated SLIPI-LIF ratio depicting the absolute temperature of the liquid in the cuvette. Results have been deduced using the SLIPI calibration curve given in Fig. 7. It is seen that the water temperature is nearly homogenous throughout the cuvette for each reference temperature case ranging between 25°C to 85°C.

5. Spray measurement results

5.1 Non-calibrated results

The CONV and SLIPI two-color LIF ratio are shown in Figs. 9(a)-9(d) and Figs. 9(e)-9(h) respectively, for droplets temperature from 25°C to 55°C. The temperature is measured within the spray by inserting a thermocouple in the calibration region indicated in (a) and (e). Each sub-image is recorded (just after removing the thermocouple) with an exposure time of 0.6 seconds and averaged over 10 exposures. The dye concentration is fixed to $\mu_e = 2.55$ cm^{-1} and the laser power along the incident light sheet is $P_1 = 35$ mW. A background image () is recorded prior to each recordings and the images of the two bands are background subtracted. This post-processing routine is operated for a fair comparison between CONV and SLIPI even though a background subtraction is not required with SLIPI. In order to avoid numerical errors while ratioing the data, any pixel value below a given threshold is discarded. This was done at thresholds of 0.01% and 1.5% of the maximum intensities of the SLIPI and CONV images, respectively. In Figs. 9(a)-9(d), it is apparent that there is an undesired signal in the non-illuminated spray regions. This unwanted signal is the result of multiple light scattering

#253552 Received 9 Nov 2015; revised 10 Feb 2016; accepted 14 Feb 2016; published 26 Feb 2016

detection. In opposition, such effects are accounted for in the SLIPI images, as shown in Figs. 9(e)-9(h). By now comparing the dynamic range of the LIF ratio between CONV and SLIPI, it can be seen that the former changes only from 0.65 to 0.90 while the later changes from 0.35 to 0.80 at temperatures ranging between 25°C and 55°C. It can be noted that the spray symmetry is well observed as the intensity division cancels out the effects of light extinction along the laser sheet and signal attenuation in between the light sheet and the camera.

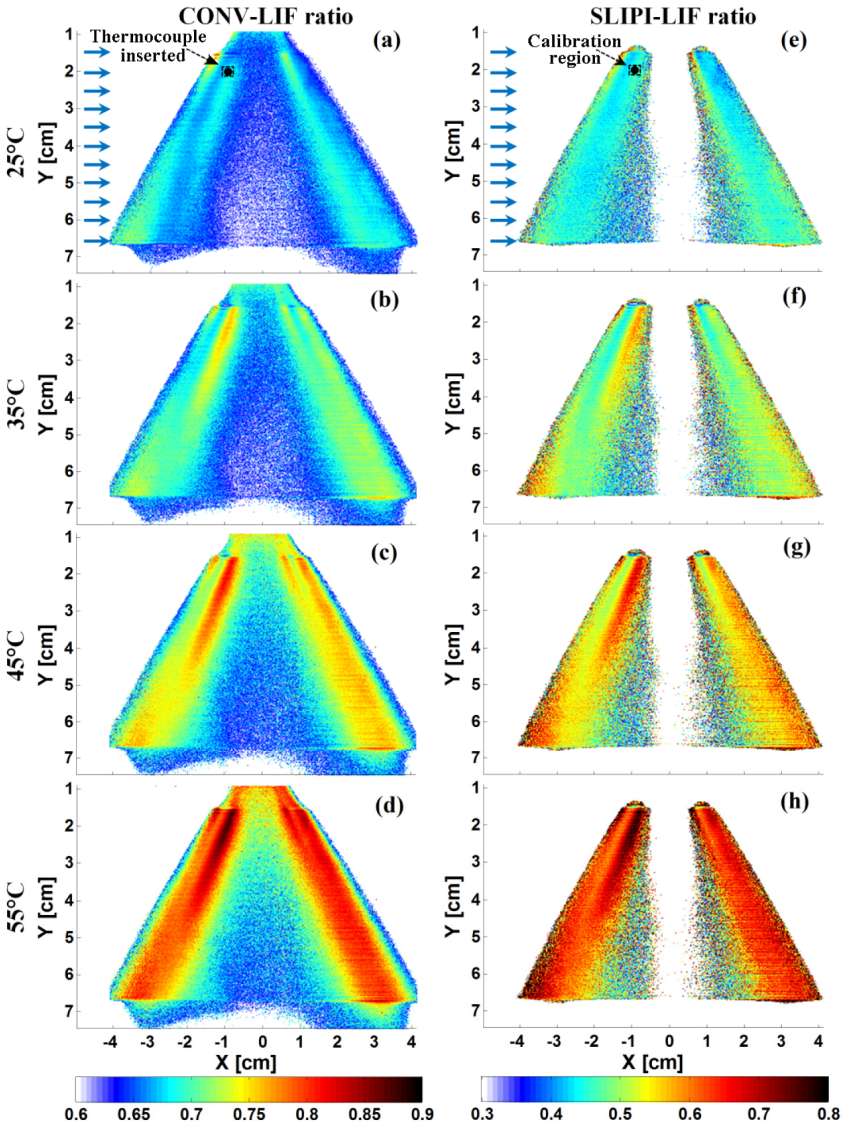

Fig. 9. Averaged non-calibrated CONV two-color LIF ratio (a-d) and SLIPI two-color LIF ratio (e-h) for temperatures of 25°C, 35°C, 45°C and 55°C. Both the detection schemes capture the changes in droplet temperature. However, in contrast to the SLIPI cases, the CONV ratio produces unexpected signals outside the illumination plane and temperature gradients are smoothed in the center of the spray due to the contribution from multiple light scattering.

The spray investigated here was at an optical depth $OD \approx 1$ only, as reported in [23]. Therefore, the effects from multiple light scattering were not severe and the conventional LIF ratio approach could still provide information regarding spray temperature. It could nevertheless be mentioned that in an optically dense medium where $OD \geq 2$, multiple light

#253552 Received 9 Nov 2015; revised 10 Feb 2016; accepted 14 Feb 2016; published 26 Feb 2016

scattering is, then, dominant, which would enhance the contribution of the unwanted surrounding light in *BG* (see Eq. (1)). In such a case the temperature gradients on the images will become not visible anymore from the CONV-LIF ratio. It can also be remarked that in the current case, the distribution of multiply scattered photons is equivalent for the two bands. This differs from ratioing a LIF and Mie images where the contribution of multiple scattering is distributed differently on the recorded images as shown in [23].

5.2 Effects of dye concentration and laser power

The SLIPI-LIF ratio images showing the effects of change in dye concentration (C) and in incident laser power (P) are given in Fig. 10 and Fig. 11, respectively. In Fig. 10, two dye concentrations, C_1 where $\mu_e = 2.55$ cm^{-1} and C_2 where $\mu_e = 0.90$ cm^{-1}, are tested at fixed laser power P = 35 mW for 25°C and 55°C liquid temperatures. By comparing Figs. 10(a) and 10(b) as well as Figs. 10(c) and 10(d), it is apparent that the ratio is not the same for the two concentrations. This is due to self-absorption effects where part of the emission is re-absorbed by the Fluorescein dye. At higher dye concentration, here for example in C_1, the self-absorption reduces especially the signal through F_1 which consequently leads to higher ratios of I_{LIF2}/I_{LIF1}. In order to correct for such discrepancies, three-color LIF approach is suggested by Lavielle *et al.* [32]. In Fig. 11, two incident laser powers, $P_1 = 35$ mW and $P_2 = 17.5$ mW, are investigated at fixed concentration C_1 for 25°C and 55°C reference temperatures. From Figs. 11(a)-11(b) and Figs. 11(c)-11(d), it is seen, in this case, that the LIF ratio is equivalent for P_1 and P_2. Therefore, the temperature response is independent, here, with the variation of the incident laser power.

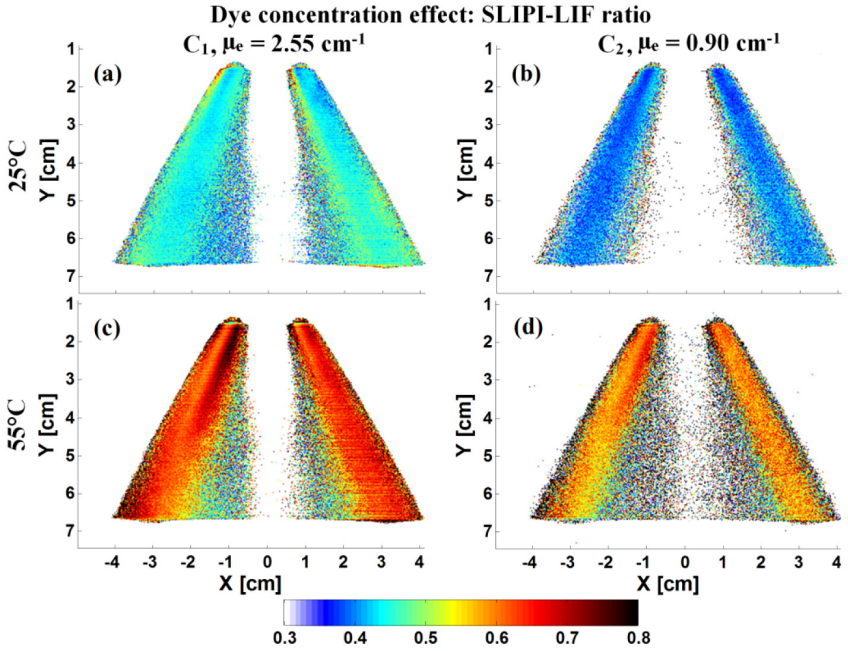

Fig. 10. Averaged SLIPI-two color LIF ratio images showing the effects of change in dye concentration C_1 to C_2 at constant laser power $P_1 = 35$mW, are given. (a, b) and (c, d) show that the LIF ratio changes with variation from C_1 to C_2 at reference temperatures 25°C and 55°C, respectively.

#253552 Received 9 Nov 2015; revised 10 Feb 2016; accepted 14 Feb 2016; published 26 Feb 2016

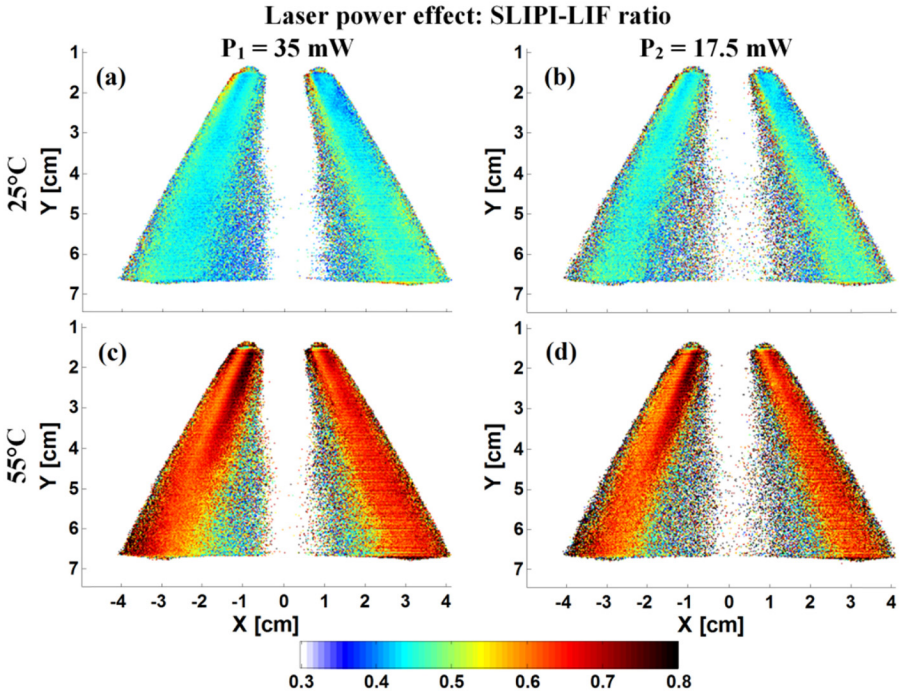

Fig. 11. Averaged SLIPI two-color LIF ratio images depicting the effects of variation in incident laser powers from P_1 = 35 mW to P_2 = 17.5 mW at fixed dye concentration C_1. (a, b) and (c, d) show that the ratio is independent of the variation from P_1 to P_2 at reference temperatures 25°C and 55°C, respectively.

5.3 Calibrated results

The calibration curve showing the SLIPI-LIF ratio as a function of droplet temperature is shown in Fig. 12. An averaged intensity ratio over an area of 20 × 20 pixels is considered, corresponding to the calibration coordinate point X = –1 cm, Y = 2 cm, where the thermocouple was inserted (as shown in Fig. 9(a)). A calibration fitting curve, here a third order polynomial, is used for converting the SLIPI-LIF ratio in droplet temperature.

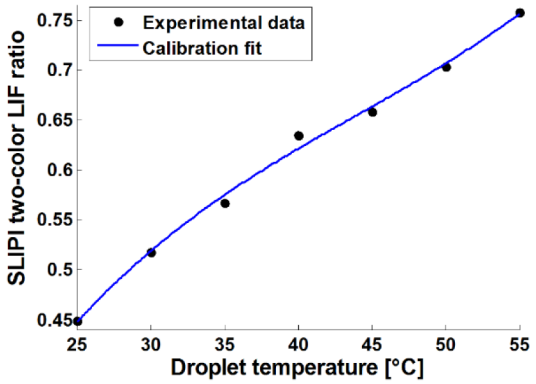

Fig. 12. The averaged SLIPI two-color LIF ratio is plotted against droplet temperature in the range of 25-55°C. This calibration curve is used to extract the absolute 2D mapping of droplet temperature shown in Fig. 13.

The two-dimensional absolute temperature mapping of the spray droplets are given in Fig. 13(a), 13(b), 13(c) and 13(d), respectively recorded at reference temperatures 25°C, 35°C,

#253552 Received 9 Nov 2015; revised 10 Feb 2016; accepted 14 Feb 2016; published 26 Feb 2016

45°C and 55°C. In (a) the droplet temperature is overall homogeneous throughout the spray and equals 25°C as expected as the injected water was at room temperature. When the injected liquid is heated-up, gradients of temperature are becoming apparent over the spray, with a cooler region in the spray center. For instance, for the case of image (d) this gradient ranges from 25°C in the hollow region of the spray to 55°C near the nozzle orifice.

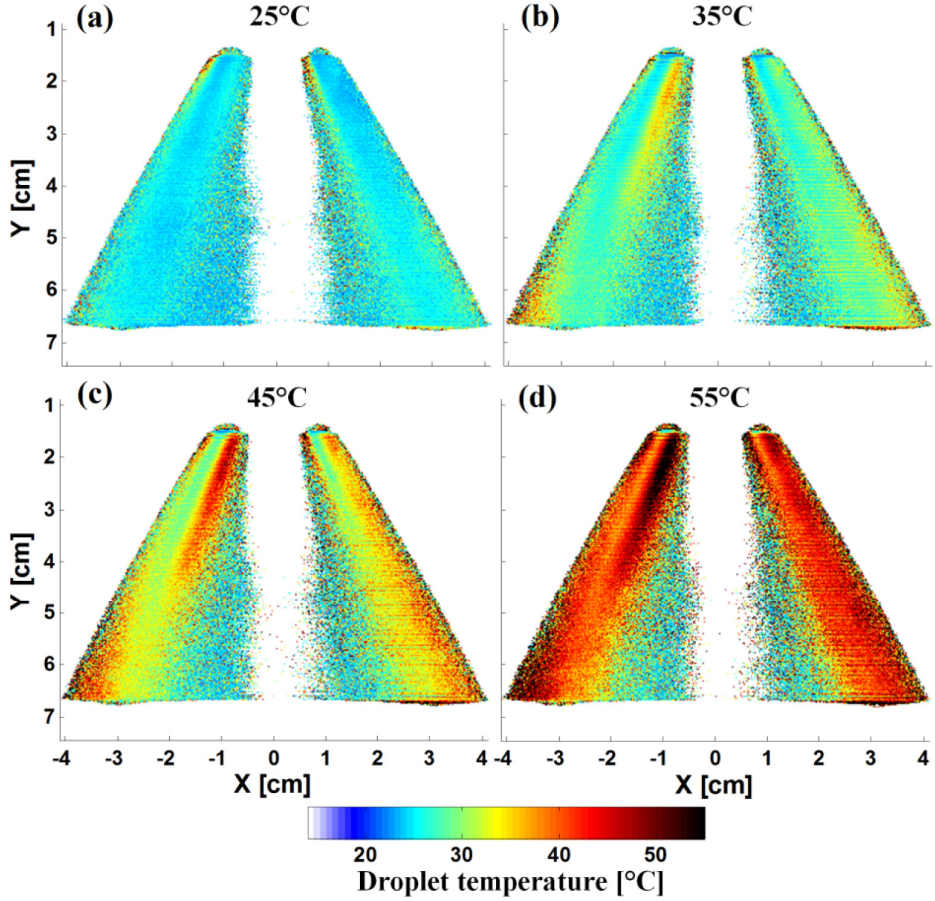

Fig. 13. Two-dimensional map of droplet temperature in a hollow-cone water spray at reference temperature varying between 25°C to 55°C. The spray cools down in its hollow region while the liquid located nearer to the nozzle orifice is hotter.

7. Conclusions

In this work, it is demonstrated that the use of structured illumination in combination with two-color LIF improves largely the sensitivity of temperature measurements in aqueous solutions and sprays. It is found, for the case of Fluorescein mixed with water, that the sensitivity can increase up to 6 times (at 85°C) by means of structured illumination. This is due to the fact that the unwanted sources of error, corresponding mainly to background fluorescence in the cuvette and multiple light scattering in sprays, can be suppressed with SLIPI. In addition to this sensitivity improvement, the suppression of the unwanted light contribution allows obtaining sharper temperature gradients. It is also found that the LIF ratio is independent of the changes in laser power between 17.5 and 35 mW. However, significant changes in the resulting ratio were observable when varying the dye concentration. This observation is due to self-absorption effects in the spectral region of 500 nm to 520 nm, where the absorption and emission spectra of Fluorescein overlap. Thus, extracting the

#253552 Received 9 Nov 2015; revised 10 Feb 2016; accepted 14 Feb 2016; published 26 Feb 2016

absolute temperature images from a common calibration curve but with different dye concentrations would lead to erroneous results. Further investigations on using different temperature sensitive dyes and/or different spectral regions of the bandpass filters will be investigated. It is finally believed, from those results, that the use of structured illumination for 2D liquid thermometry purposes is a promising future approach.

Acknowledgments

The authors would like to thank Dr. Lars Zigan and Prof. Stefan Will from the Institute of Engineering Thermodynamics, Erlangen for co-supervising Stephanie Polster's master thesis work. This project has received funding from the European Research Council (ERC) under the European Union's Horizon 2020 research and innovation programme (Agreement No 638546 - ERC starting grant "Spray-Imaging"). The Swedish Research Council is also acknowledged for providing the financial support for the Project 2011-4272.

#253552 Received 9 Nov 2015; revised 10 Feb 2016; accepted 14 Feb 2016; published 26 Feb 2016